



## Sensitivity Analysis of Design Variables for Self-centering Buckling Restrained Braces with Shape Memory Alloys

Wilson Carofilis<sup>1\*</sup>, Eugene Kim<sup>2</sup> and Donghyuk Jung<sup>3</sup>

<sup>1</sup>PhD Student, Department of Civil & Environmental Engineering, University of Waterloo, Waterloo, ON, Canada

<sup>2</sup>Assistant Professor, Department of Civil & Environmental Engineering, University of Waterloo, Waterloo, ON, Canada

<sup>3</sup>Assistant Professor, School of Civil, Environmental & Architectural Engineering, Korea University, South Korea

\*[wcarofil@uwaterloo.ca](mailto:wcarofil@uwaterloo.ca)

### ABSTRACT

Self-centering buckling restrained braces (SCBRBs) equipped with shape memory alloys (SMAs) have the ability to significantly reduce residual deformations and structural damage during seismic events. The design of these devices is governed mainly by the mechanical properties of the SMA and steel core. The prestressed SMA provides the self-centering effect, while the yielding of the steel core contributes to energy dissipation. Currently, the values of some design parameters (e.g., post-yield stiffness ratio factor, compression strength, and strain hardening adjustment factors) are recommended in the literature, but it is not fully understood how their variation influences the modelling of the seismic response of structures. In this study a sensitivity analysis is conducted on the variables controlling the design of self-centering buckling restrained braces with SMAs. Conducting this sensitivity analysis serves to optimize the values for these input variables so that a more effective design can be attained. Firstly, a cyclic analysis is conducted to examine the hysteretic behavior of an isolated brace. Subsequently, non-linear dynamic analyses are performed for a three-story moment resisting steel frame equipped with SCBRBs. The building response is evaluated in terms of peak story drift, peak floor acceleration, and residual drift for the design earthquake. These demand parameters are also used to quantify the seismic performance of non-structural elements. The outcomes are illustrated through a tornado diagram where it is demonstrated that self-centering and energy dissipation capacity are mostly affected by the properties of the SMA. Additionally, the residual story drift is sensitive to changes in the post-yield stiffness ratio factor and SMA properties. It is expected that these outcomes will help guide users to optimize the design of these systems by selecting the inputs variables to attain a specific level of absorbed energy and self-centering capability.

Keywords: self-centering, energy dissipation, design parameters, sensitivity analysis, seismic behavior

### INTRODUCTION

Self-centering buckling-restrained braces (SCBRBs) have been gaining popularity as a retrofit measure in conventional moment resisting frame systems since they can promote better seismic resilience levels. SCBRBs have superior performance than regular bracing systems and conventional buckling restrained braces (BRBs) [1] given their combined ductile behavior (i.e., energy dissipation capacity) and self-centering effect (i.e., restoring undeformed conditions). The self-centering action is achieved through prestressing of high strength materials. Shape memory alloys (SMAs) are practical for structural seismic applications due to their unique thermomechanical properties known as superelasticity and shape memory effect (i.e., recovery of undeformed configuration upon heating). Some studies [2-4] have explored the self-centering effect by means of super-elastic SMA. For example, Miller et al. [2] devised a SCBRB with nickel-titanium based SMA (NiTi-SMA) tendons that achieved satisfactory performance. Recently, Carofilis et al. [5] carried out a numerical study to increase the resilience of a moment resisting steel frame building equipped with SCBRBs that utilizes iron-based SMA (Fe-SMA). This study conceptualized a low-cost SCBRB in which the self-centering action is provided by prestressed Fe-SMA tendons. The prestressing is achieved through the heat-activated shape memory effect of the Fe-SMA.

The ability to return to a pre-loading state is the most significant feature of SCBRBs since it can considerably reduce structural damage and permanent deformations in a structure. Residual deformations are an important metric in earthquake engineering for determining the reparability of a structure. Residual lateral deformation (e.g., residual drifts) and inelastic damage to

structural components can make it more economically advantageous to demolish a building after an earthquake rather than invest resources to repair them [6]. SCBRBs can increase the likelihood that a building will be in a reasonably repairable state after an earthquake, thus improving resilience.

In addition to the restoring effect, SCBRBs also include an energy dissipative steel core responsible for the energy absorption (hysteretic behavior) under dynamic actions. The steel core provides the ductile behavior and transmit the axial forces to other member components. Earthquake energy is absorbed through the yielding of this component which is restrained by an outer steel tube that prevents the steel core from buckling and allows the brace to yield even under compression.

The overall performance of SCBRBs and the seismic response of buildings equipped with these devices is directly influenced by the self-centering effect and energy dissipation of SCBRBs. Several parameters control the design of SCBRBs, and the selection of optimum values can affect the seismic response of buildings. Eatherton et al. [3] performed 147 numerical simulations of SCBRBs subjected to cyclic loading to study the variables controlling their performance and experimentally evaluated the behavior of 15 SCBRB prototypes. Their study focused on four primary design variables: brace axial capacity, self-centering ratio, SMA initial pretension stress and SMA gage length with special emphasis on the self-centering ratio and prestressing level of the SMA. Even though this study investigated the variation of these metrics, it is not clear how the overall behavior the SCBRBs is affected by other parameters not considered by Eatherton et al. [3] such as the modulus of elasticity of the SMA and mechanical properties of the steel core. Further exploring these design variables can assist in understanding what metrics impact energy absorption characteristics during seismic actions and potentially reduce the efficacy of SCBRBs. Similarly, large permanent residual deformations may be enlarged in a building which limits the action of SCBRBs, reducing their performance and getting a similar behavior to regular BRBs.

### CASE STUDY BUILDING

A three-story 2D moment-resisting steel frame was selected as the case-study building to investigate the effect of varying SCBRB design parameters on the global seismic response. More details on the numerical model can be found in Chalarca [7] and FEMA 440 [8]. Figure 1 shows the steel sections and geometry adopted in the numerical model developed in OpenSees [9]. The initial design of the SCBRB system was carried out through an equivalent static method assuming 75% of the lateral action is resisted by the brace system. The lateral force was determined through the vertical distribution of seismic forces described by ASCE 7-16 [10]. The fundamental period of the braced structure was estimated using the Eq. (1)

$$T_a = C_t h_n^x \tag{1}$$

Where  $C_t$  and  $x$  are building period coefficients and set as 0.0731 and 0.75, respectively (i.e., steel buckling-restrained braced frames option) and  $h_n$  is the total height of the building taken as 11,880 mm, resulting in a fundamental period ( $T_a$ ) of 0.47 seconds. The FEMA P-695 [11] far-field ground motion set composed of 44 records representing the seismicity of western United States was scaled such that the median spectral acceleration at a period of one second matches the ASCE 7-16 design spectrum for the city of Los Angeles (soil type D). According to the design spectrum for the design earthquake (DE) shown in Figure 1, the design spectral acceleration associated with the fundamental period of 0.47 seconds is 1g. The response reduction factor ( $R$ ) was taken as 8, which is suggested for BRB systems [10].

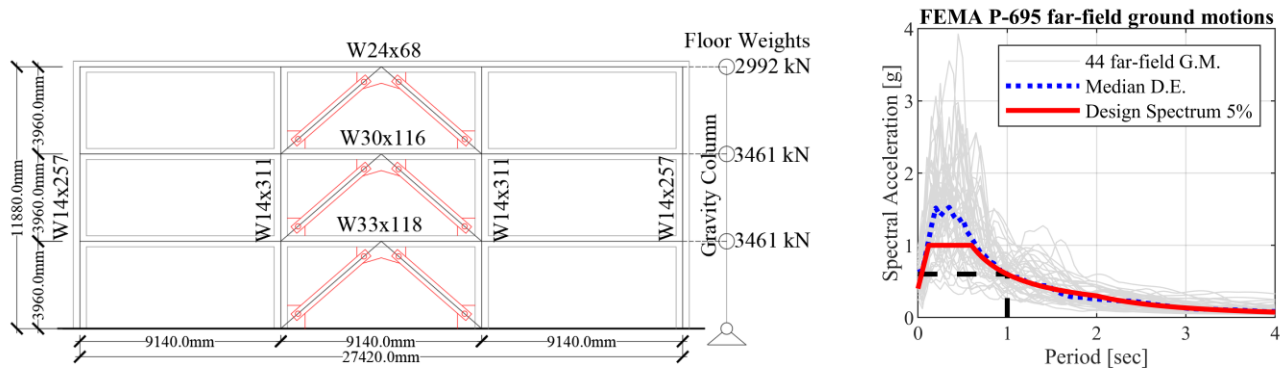


Figure 1. Case-study building with brace configuration and design response spectrum.

### SCBRB DESIGN

The design approach of the SCBRB system adopted for this study is based on the prototype of Miller et al. [2]. As illustrated in Figure 2, the SCBRB is composed of a middle and outer tubes welded to the core at opposite ends to allow the brace to always work in tension and activate the restoring force from the prestressed SMA tendons. The pre-tensioned SMA tendons

are connected to the BRB through free-floating end plates on the concentric steel tubes. The anchorage plates have cruciform shaped slots that enable the BRB core and tubes to move freely since the plates are not connected (welded) neither to the BRB core nor tubes. The SCBRB behavior is attained by combining the self-centering effect that comes from the prestressing of SMA tendons with the hysteretic behavior of the steel core as illustrated in Figure 2.

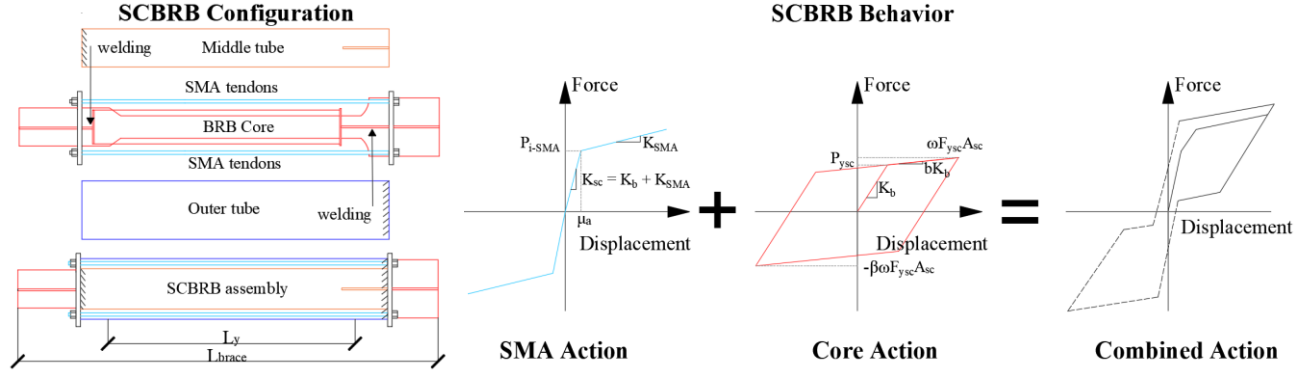


Figure 2. SCBRB configuration and hysteresis curve.

The modelling parameters are also indicated in Figure 2, which shows the isolated actions for the SMA and steel core. For the SMA action the modelling parameters are the initial prestressing force of the SMA tendons ( $P_{i-SMA}$ ), the total stiffness of the brace system ( $K_{sc}$ ), the stiffness of the SMA tendons ( $K_{SMA}$ ), and the displacement activating the restoring force in the brace ( $\mu_a$ ). Whereas the steel core includes the modelling variables yielding force of the steel core ( $P_{ysc}$ ) and the initial stiffness of the steel core ( $K_b$ ). The combined action of these design parameters (i.e., overall SCBRB behavior) is affected by the design variables  $\alpha_{sc}$  that defines the separation between the initial SMA pretension force and the strain hardened steel core force (also known as the self-centering ratio [3]),  $\beta$  the compression strength adjustment factor for the steel core,  $\omega$  the strain hardening adjustment factor for the steel core,  $A_{sc}$  the cross-section area of the steel core,  $F_{ysc}$  yielding stress in the steel core,  $F_{i-SMA}$  prestressing stress of the SMA tendons, and  $E_{SMA}$  modulus of elasticity of the SMA. These design variables were considered for the sensitivity analysis to assess how their variability impact the modelling parameters of Figure 2.

The modelling variables are related to the design parameters through the following expressions. For the initial stiffness of the steel core, it was assumed an effective length of the brace as 70% of the work-point-to-work-point distance as recommended in NIST GCR 10-917-8 [1]. FEMA P795 [12] suggests that the effective stiffness of the brace can be represented as the in-series sum of the individual element stiffnesses, consisting of the steel core (yielding portion), stiffness of the connection portions, and the stiffness of the transition portions. However, Nippon Steel Engineering [13] proposed the simplified relationship shown in Eq. (2) which was used to approximate the total stiffness of a brace solely based on the stiffness of the steel core.  $L_y$  is the yielding length, and  $E_s$  is the steel modulus of elasticity.

$$K_b \cong 0.83 \frac{A_{sc} E_s}{L_y} \quad (2)$$

The yielding force in the steel core ( $P_{ysc}$ ) and initial SMA prestressing force ( $P_{i-SMA}$ ) are related through Eq. (3). They represent the axial capacity ( $\phi P_n$ ) of the brace and must be greater or equal to the axial demand  $P_u$ . The axial strength reduction factor is taken as 0.9 for both tension and compression. The steel core yielding force and SMA pretension force can be related through Eq. (4) based on ANSI/AISC 341-16 seismic provisions [14].

$$\phi P_n = \phi (P_{ysc} + P_{i-SMA}) = 0.9 (F_{ysc} A_{sc} + F_{i-SMA} A_{SMA}) \geq P_u \quad (3)$$

$$F_{i-SMA} A_{SMA} = \alpha_{sc} \beta \omega F_{ysc} A_{sc} \quad (4)$$

The required cross-sectional areas for the steel core and SMA can be determined using Eq. (5) and Eq. (6) respectively.

$$A_{sc} = \frac{P_u}{\phi F_{ysc} (1 + \alpha_{sc} \beta \omega)} \quad (5)$$

$$A_{SMA} = \frac{\alpha_{sc} \beta \omega F_{ysc} A_{sc}}{F_{i-SMA}} \quad (6)$$

The initial stiffness of the SCBRB system ( $K_{sc}$ ) is a combination of the stiffness of the steel brace and the stiffness of the prestressed SMA ( $K_{SMA}$ ) which can be determined by Eq. (7). Once the prestressing force of the SMA ( $P_{i-SMA}$ ) is exceeded or when the deformation in the brace is larger than  $\mu_a$  (Eq. 8) the stiffness of the device decreases and is governed solely by the restoring action of the SMA tendons. In the case of the steel core, the brace starts absorbing energy once the core yields and undergoes plastic deformations. The post-yield stiffness of the brace core is assumed to be 10% of the initial stiffness ( $K_b$  in Figure 2).

$$K_{SMA} = \frac{E_{SMA}A_{SMA}}{L_y} \quad (7)$$

$$\mu_a = \frac{P_{i-SMA}}{K_b + K_{SMA}} \quad (8)$$

The behavior of the SCBRBs was modelled in OpenSees [9] by combining two uniaxial materials as illustrated in Figure 2. The self-centering action was represented by a ElasticBilin uniaxial material while the Steel01 uniaxial material was adopted for the elastoplastic behavior of the steel core. These two materials were combined in parallel to obtain the overall behavior of the SCBRBs.

### SENSITIVITY ANALYSIS

Sensitivity analysis using the tornado diagram technique was used to study the effect of varying the SCBRB design parameters on the global seismic response of the case study building. The analysis was conducted by first setting all considered design variables to their established median values. Subsequently, each parameter is varied in magnitude one at a time while the other variables are constrained. The value of each variable was incremented as a fraction of their median values (i.e., 50%, 75%, 90%, 110%, 125%, and 150%). The design variables considered are  $\alpha_{sc}$ ,  $\beta$ ,  $\omega$ ,  $F_{y_{sc}}$ ,  $F_{i-SMA}$ ,  $E_{SMA}$ , and  $A_{sc}$  as presented in the previous section. The tornado diagrams relate the sensitivity of  $P_{y_{sc}}$ ,  $K_b$ ,  $K_{sc}$ ,  $K_{SMA}$ , and  $\mu_a$  to these design variables.

The initial median values adopted for the design variables are based on recommendations provided in the literature. For example, Miller et al. [2] states that it is desirable for the initial SMA pretension force to be greater than the yield force of the steel core to achieve full self-centering behavior. Therefore,  $\alpha_{sc}$  should be set as at least one. Furthermore, Miller et al. [2] recommends typical values of  $\beta = 1.20$  and  $\omega = 1.35$  which were adopted as the reference values (median values) to conduct this sensitivity analysis. Eatherton et al. [3] suggest similar values for these variables ( $\beta = 1.08$  and  $\omega = 1.25$ ). In the case of  $\alpha_{sc}$ , Eatherton et al. [3] suggest setting this variable equal to 1 can overcome the resistance provided by the strain hardened in the brace, but significant prestress in the SMA tendons can be lost. Values for  $\alpha_{sc}$  between 0.5 and 1.5 control residual drifts and limit brace overstrength. Overstrength can be reduced by adopting a large value for  $\alpha_{sc}$  with larger initial SMA stress. Ratios larger than 0.5 can eliminate residual elongations in the brace but it not necessary to adopt  $\alpha_{sc}$  larger than 2 given that much lower values can control/mitigate residual deformation in the brace system. For the other parameters, several studies have addressed the relevant properties of SMA [15,16]. The recommended ranges for  $F_{i-SMA}$  and  $E_{SMA}$  are 200-600MPa and 70-170GPa, respectively [17,18] whereas  $F_{y_{sc}}$  depends on the type of steel adopted and ranges between 200-345 MPa [1], and  $A_{sc}$  is derived through Eq. (4). Table 1 lists the median values of the design parameters adopted for this study.

Table 1. Median values adopted for the design variables of SCBRB.

Parameters	$\alpha_{sc}$	$\beta$	$\omega$	$F_{y_{sc}}$	$F_{i-SMA}$	$E_{SMA}$
Value	1.0	1.2	1.35	250 MPa	300 MPa	80 GPa

The results of the sensitivity analysis are shown by the tornado diagrams in Figure 3. The horizontal bars represent the lower and upper bound variation (i.e., 50% and 150% of the median value) of the design variables with respect to each modelling parameter. Reduction in a design parameter is depicted with red color, whereas increase is illustrated by blue color. The yielding force of the steel core ( $P_{y_{sc}}$ ) is most significantly influenced by variation of its cross-sectional area ( $A_{sc}$ ). These two variables are linearly related as shown in Eq. (3). The design parameters  $\alpha_{sc}$ ,  $\beta$ ,  $\omega$  also affect  $P_{y_{sc}}$  and can delay the hysteresis behavior of the brace. If these parameters decrease considerably in magnitude, then  $P_{y_{sc}}$  increases substantially. Changes in  $E_{SMA}$  and  $F_{i-SMA}$  have no impact over  $P_{y_{sc}}$  since the behavior of the steel core is not related to these properties. Even though the yield strength of the steel core ( $F_{y_{sc}}$ ) relates directly to  $P_{y_{sc}}$ ,  $F_{y_{sc}}$  is part of the denominator of  $A_{sc}$  in Eq. (5), and thereby when calculating  $P_{y_{sc}}$ ,  $F_{y_{sc}}$  cancels out. In the case of the stiffness of the steel core ( $K_b$ ), this design variable is controlled by  $F_{y_{sc}}$  since any increasing in magnitude makes  $K_b$  smaller. As specified in Eq. (2),  $K_b$  depends on  $A_{sc}$ , but  $A_{sc}$  is inversely associated to  $F_{y_{sc}}$ . Consequently, decreasing  $F_{y_{sc}}$  results in larger  $A_{sc}$  and  $K_b$ . The factors  $\alpha_{sc}$ ,  $\beta$ ,  $\omega$  also affect  $K_b$ , but their impact is less critical. Again, design parameters that are not related to the properties of the steel core (i.e.,  $E_{SMA}$  and  $F_{i-SMA}$ ) have no influence on  $K_b$ . The total stiffness of the brace ( $K_{sc}$ ) is affected by all design variables.  $K_{sc}$  is directly related to both the cross-sectional area of the steel core and  $E_{SMA}$  (i.e., variation of  $K_{sc}$  depends on the increase or decrease of these two parameters), but the influence of  $E_{SMA}$  is smaller than that of  $A_{sc}$ . A similar trend is produced by the parameters  $\alpha_{sc}$ ,  $\beta$ ,  $\omega$ , but their impact is more notorious when they

decrease, which makes the SCBRB stiffer. The reduction in  $F_{i-SMA}$  and  $F_{y-sc}$ , significantly increases the stiffness of the brace, meaning that lower prestressing in the SMA and yield strength transfer more stiffness to the brace. Furthermore, the stiffness of the SMA tendons is strongly affected by the prestressing stress  $F_{i-SMA}$ . When  $F_{i-SMA}$  decreases, the stiffness is increases considerably.  $E_{SMA}$  and  $A_{sc}$  are linearly related to  $K_{SMA}$  as indicated by Eq. (7) and (6). Finally, the displacement ( $\mu_a$ ) that activates the restoring force is equally affected by  $F_{y-sc}$ ,  $\alpha_{sc}$ ,  $\beta$ ,  $\omega$ . Unlike  $F_{i-SMA}$ ,  $E_{SMA}$  is inversely related to  $\mu_a$  as  $\mu_a$  decreases when  $E_{SMA}$  increases. In other words, the restoring force in the SCBRB can be activated with a much lower displacement.

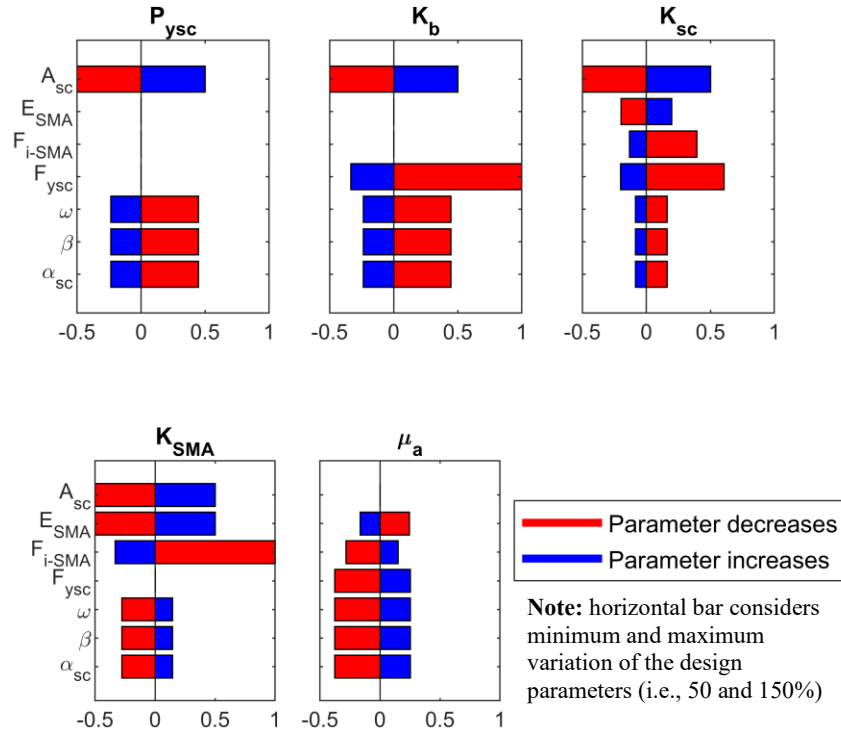


Figure 3. Tornado diagram of variables influencing the design of SCBRBs.

### Single brace analysis

The impact of the design variables over the cyclic behavior of the brace is presented in this section. The results correspond to the lower and upper bounds (i.e., 50% and 150% of the median values) of the brace placed in the first story. The hysteretic behavior is illustrated in Figure 4. There is not much variation of the hysteresis curve when the design parameters  $\alpha_{sc}$ ,  $\beta$ ,  $\omega$  are modified, just a small decrease in the post-yielding stiffness. In the case of  $F_{y-sc}$ , a similar behavior is observed among all hysteresis curves with only a small increase in the post-yielding stiffness when  $F_{y-sc}$  is reduced. Similarly, reduction of  $F_{i-SMA}$  causes an increasing trend in the branch associated with the restoring force. A substantial increase is achieved when  $F_{i-SMA}$  decreases by 50%, meaning that a larger recovery stress is needed to restore the undeformed condition in the brace.  $E_{SMA}$  and  $A_{sc}$  are directly related to the hysteretic behavior of the brace. Increasing  $E_{SMA}$  increases the post-secondary stiffness and a reduction in  $E_{SMA}$  reduces the stiffness. The same pattern is observed for  $A_{sc}$ , but with a stronger effect.

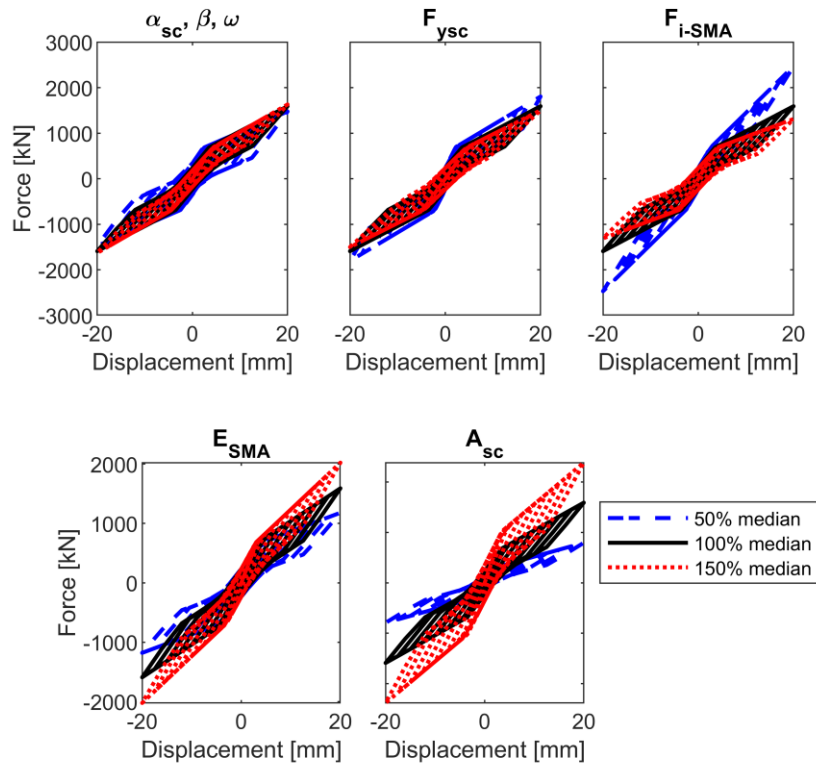


Figure 4. Hysteresis behavior variation of a single brace.

The absorbed energy gives a better idea of how the variation of the design parameters affect the cyclic response of the brace. As observed in Figure 5, the least influential parameters are  $\alpha_{sc}$ ,  $\beta$ ,  $\omega$  since the absorbed energy remains almost unchanged. Gradual variation in the absorbed energy is observed for the other parameters. Small variations in the absorbed energy are generated by changes to  $F_{ysc}$ , while the other variables substantially affect the amount of absorbed energy. For example, limiting the prestress level to values around 200 MPa (approximately 67% of 300 MPa) can almost double the absorbed energy compared to a prestress of 300 MPa. In contrast, increasing  $E_{SMA}$  above 100% increased the energy dissipation in the brace while values lower than 40 GPa (50% of  $E_{SMA}$ ) considerably reduced the absorbed energy. Finally, the cross-section ( $A_{sc}$ ) of the steel core directly impacts the absorbed energy of the SCBRB. If a larger  $A_{sc}$  is implemented, the amount of dissipated energy achieved increases linearly according to median value of  $A_{sc}$ .

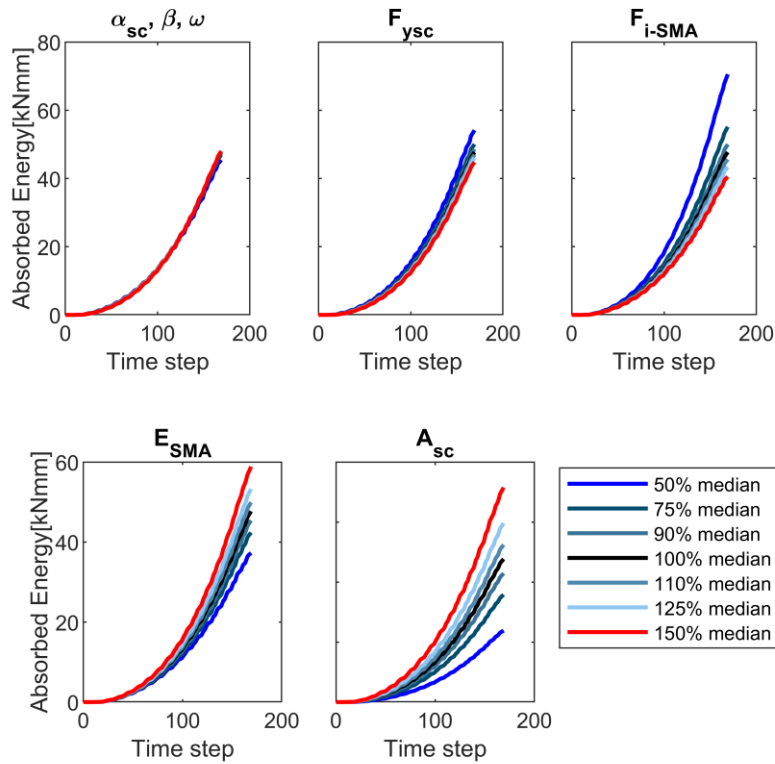


Figure 5. Absorbed energy variation of a single brace.

The variation of the design parameters also affects the residual deformation in the SCBRB as illustrated in Figure 6. The residual deformation increases by decreasing the parameters  $\alpha_{sc}$ ,  $\beta$ ,  $\omega$ . In fact, a gradual increase is expected when these variables are reduced by up to 50%. A similar behavior is expected for  $E_{SMA}$ , but its impact is less significant. Furthermore, changes to  $F_{ysc}$  and  $F_{i-SMA}$  present a direct influence on the residual deformation (increasing or decreasing depending on the magnitude of these variables), although the increasing of these variables does not increase the residual deformation in the brace considerably. The cross-section of the steel core has no influence over the residual deformation of the brace. Overall, to obtain a substantial reduction of the residual deformation in the brace, the parameters  $\alpha_{sc}$ ,  $\beta$ ,  $\omega$  can be reduced or  $E_{SMA}$  increased.

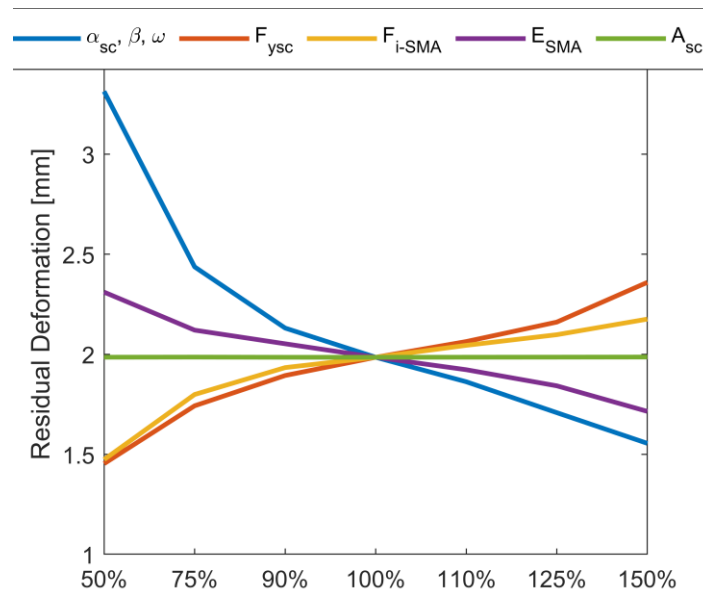


Figure 6. Residual deformation variation of a single brace.

The variation and impact of  $\alpha_{sc}$  on the behavior of the SCBRB is in agreement with the findings of Eatherton et al. [3]. Eatherton et al. [3] found that  $\alpha_{sc}$  affect the energy dissipation and that systems with minimal energy dissipation can be expected to create similar ductility demands as conventional BRB systems. It is likely that no permanent deformation is produced in the brace when setting  $\alpha_{sc}$  to 1.0, although as observed here reducing  $\alpha_{sc}$  reaches a considerably reduction of the SCBRB deformation.

### SCBRB frame building response

The parametric study on a single brace provides a useful insight into how the different design parameters affect the behavior of an SCBRB at the member level. However, a system-level investigation is also needed to understand the impact of the variables on building response. Figure 7 shows how the natural periods of vibration of the braced frame changes according to the fluctuation of the design parameters. As the variables  $\alpha_{sc}$ ,  $\beta$ ,  $\omega$ ,  $F_{ysc}$ ,  $F_{i-SMA}$  increase in magnitude, they directly influence the dynamic properties a building by enlarging the period of vibration as observed in Figure 7. If these variables increase or decrease, the periods will follow the same behavior. When  $F_{ysc}$  changes, it is observed a substantial variation of the fundamental period. In fact, this parameter impacts the dynamic properties the most with respect to the other design variables. In contrast,  $E_{SMA}$ ,  $A_{sc}$  represent an inverse relationship with the periods of vibration. This means that low values or  $E_{SMA}$ ,  $A_{sc}$  increase the periods.

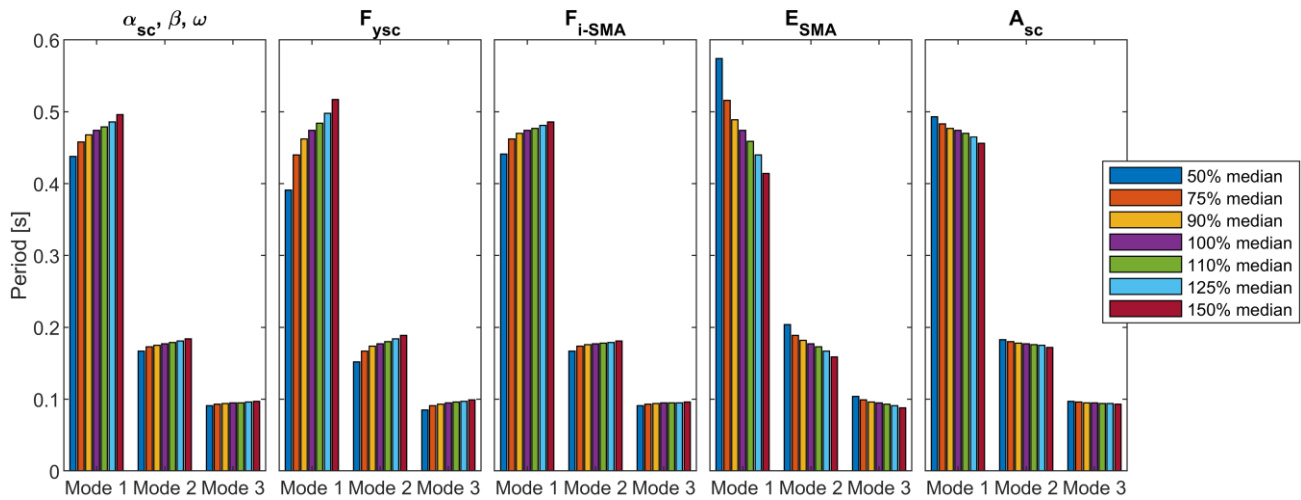


Figure 7. Variation of the dynamic properties of the case-study building.

Figure 8 illustrates changes of the median peak floor accelerations (PFAs) along each story. The variation in magnitude of the parameters  $\alpha_{sc}$ ,  $\beta$ ,  $\omega$ ,  $F_{ysc}$  seems to not severely impact the floor accelerations since PFAs are identical in magnitude. On the other hand,  $E_{SMA}$  and  $A_{sc}$  have a stronger effect on PFAs, this influence is proportional to the increase or decrease of these variables. It may be beneficial to reduce  $E_{SMA}$  and  $A_{sc}$  to lower down the magnitude of PFAs, which brings a positive effect over acceleration sensitive nonstructural elements. It is also worth commenting that  $F_{i-SMA}$  considerably increase PFAs when this parameter is reduced in half of its value, meaning that a larger restoring stress is produced which increases floor accelerations.

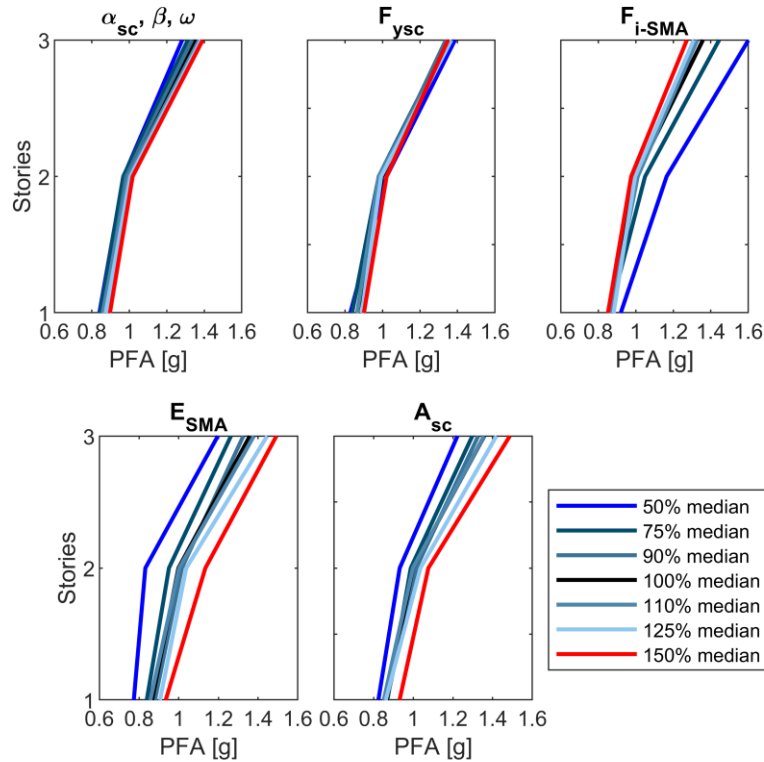


Figure 8. Variation of median PFAs for the case-study building.

Figure 9 illustrates the variation of the median peak story drift (PSD); all the design variables alter the magnitude of the story displacements and thereby PSDs. The PSDs are amplified by the increase of the parameters  $\alpha_{sc}$ ,  $\beta$ ,  $\omega$ ,  $F_{ysc}$  but an inverse trend it is observed for  $E_{SMA}$  and  $A_{sc}$ .  $E_{SMA}$  impacts PSDs the most, the extreme bounds considerably increase or reduce PSD. However, to attain a substantial decrease of this metric  $E_{SMA}$  should be increased around 50% of its median value.

Figure 10 illustrates the variation of median residual drift (RD). This is one of the most important seismic demand metrics that describes the effectiveness of SCBRB systems. The RDs slowly increase as parameters  $\alpha_{sc}$ ,  $\beta$ ,  $\omega$ ,  $F_{ysc}$  and  $A_{sc}$  are enlarged. However, the magnitudes of the RDs are extremely low compared to PSD. In fact, very small RD ( $< 0.1\%$  [3]) can typically be neglected since they do not represent a hazard for the stability/safety of a building. Finally,  $E_{SMA}$  and  $A_{sc}$  have an inverse impact on RD. Overall, increasing the magnitude of these two variables can have a positive effect on the reduction of RDs.

The outcomes found for seismic response of the braced buildings share are similar to the study of Eatherton et al. [3]. Especially for the peak drift which tend to increase with the increase of  $\alpha_{sc}$  since the among of hysteretic energy goes down. Adopting  $\alpha_{sc} \geq 0.5$  is beneficial for limiting residual drift. Moreover, ranging  $\alpha_{sc}$  from 0.75 to 2.0 can produce full self-centering behavior. Furthermore, SCBRB are able to dissipate sufficient energy even with large self-centering ratios because the SMA can also dissipate seismic energy when the restoring force is activated. For this reason, these two variables influence the amount of dissipated energy in the brace. Finally, because increases in SMA stress during earthquake motions can create significant overstrength and require larger sections for surrounding framing, the most efficient SCBRB frame designs should use low  $\alpha_{sc}$  (0.5-1.5) or use larger initial SMA stress to limit the area of the SMA component.

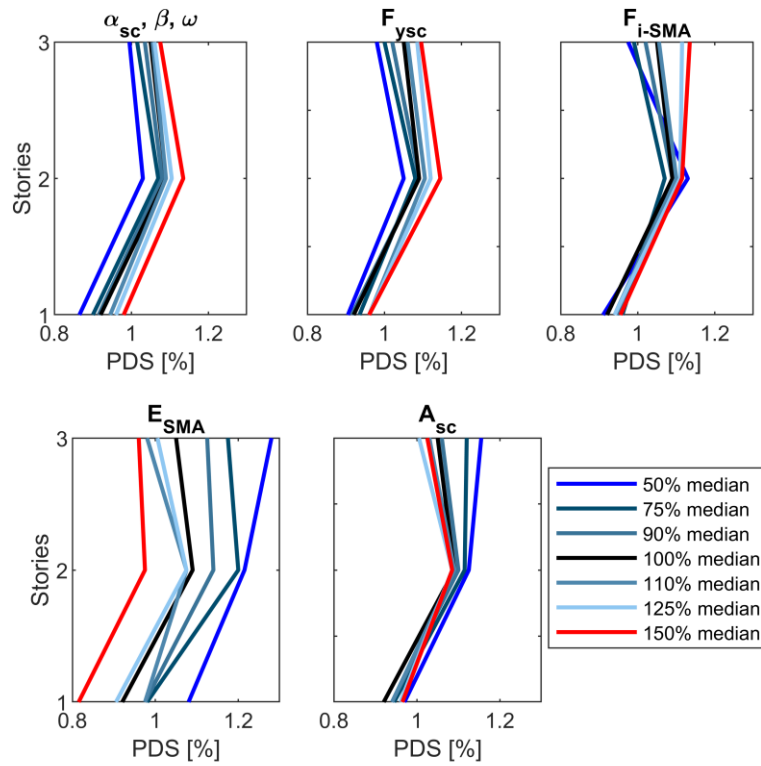


Figure 9. Variation of median PSDs of the case-study building.

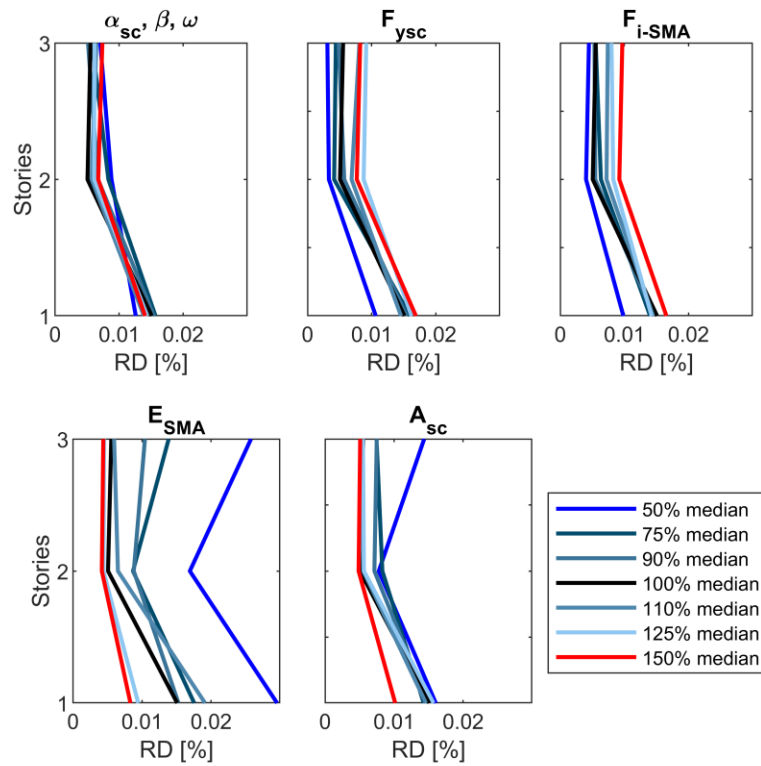


Figure 10. Variation of median RDs of the case-study building.

## CONCLUSIONS

In this study a sensitivity analysis was conducted to determine the influence of seven key design parameters on the behavior of self-centering buckling restrained braces with shape memory alloys (SMAs). The main conclusions are summarized below.

- The parameters affecting the most the self-centering action in the brace are the initial prestressing stress of the SMA, the modulus of elasticity of the SMA, the yielding stress and cross-section area of the steel core. Whereas the variables related to the self-centering ratio, compression strength adjustment factor and the strain hardening adjustment factor have a minor inverse impact.
- The energy dissipation depends mainly on the properties of the steel core, meaning the cross-section area and yielding stress are the most critical variables affecting the amount of energy absorbed by the brace. However, the absorbed energy is also affected by the mechanical properties of the SMA since SMA provides some energy dissipation.
- In terms of the overall seismic response of braced buildings, the yielding stress of the steel core, modulus of elasticity of the SMA, cross-section of steel core, and initial prestress of the SMA, alter considerably the floor accelerations in a building. On the other hand, story drifts and residual drifts are affected by all design parameters, but the modulus of elasticity of the SMA has the greatest influence.
- The initial prestress of the SMA can have a negative impact in the energy and residual deformation of the brace, as well as in the residual drift of a building when this parameter increases. However, this can also decrease the floor accelerations.
- Large modulus of elasticity of the SMA can reduce considerably drifts (maximum and permanent ones) but will increment floor accelerations. Likewise, this variable has a positive effect on the reduction of residual deformation in the brace.
- Lower values of self-centering ratio have no severe impact over the behavior of the brace and floor accelerations but can reduce story displacements. Additionally, it can enlarge not only permanent deformation in the brace but also in a building.

## REFERENCES

- [1] NIST. (2015). *Seismic design of steel buckling-restrained braced frames: a guide for practicing engineers*, GCR 15-917-34, NEHRP Seismic Design Technical Brief No. 11, produced by the Applied Technology Council and the Consortium of Universities for Research in Earthquake Engineering for the National Institute of Standards and Technology, Gaithersburg, MD.
- [2] Miller, D.J., Fahnestock, L.A. and Eatherton, M.R. (2012). "Development and experimental validation of a nickel-titanium shape memory alloy self-centering buckling-restrained brace". *Engineering Structures*, 40, 288-298, <http://dx.doi.org/10.1016/j.engstruct.2012.02.037>.
- [3] Eatherton, M.R., Fahnestock, L.A., and Miller, D.J. (2014). "Computational study of self-centering buckling-restrained braced frame seismic performance". *Earthquake Engineering & Structural dynamics*, 43, 1897-1914, DOI: 10.1002/eqe.2428.
- [4] NourEldin M., Naeem A., and Kim J. (2019). "Life-cycle cost evaluation of steel structures retrofitted with steel slit damper and shape memory alloy-based hybrid damper". *Advances in Structural Engineering*, 22(1), 3-16.
- [5] Carofilis, W., Kim, E., Jung, D., and Pinargote, J. (2022). "Numerical evaluation of self-centering buckling-restrained braces with prestressed iron-based shape memory alloy tendons". *CSCE 2022 Annual Conference*, Whistler, British Columbia.
- [6] Almufti, I. and Willford, M. (2013). *REDi rating system, resilience-based earthquake design initiative for the next generation of buildings*. Version 1.0.
- [7] Chalarca, B. (2022). *Implementation of fluid viscous dampers as a seismic protection system and its effects on the structural and nonstructural seismic response*, Doctoral thesis, University School for Advanced Studies IUSS Pavia, Italy.
- [8] FEMA. (2005). *Improvement of nonlinear static seismic analysis procedures*, FEMA 440, Federal Emergency Management Agency. United States.
- [9] McKenna, F., Scott, M.H. and Fenves, G.L. (2010). "Nonlinear finite-element analysis software architecture using object composition". *Journal of Computing in Civil Engineering*, 24(1), 95-107.
- [10] ASCE. (2017). *Minimum design loads and associate criteria for buildings and other structures*, ASCE/SEI 7-16, American Association of Civil Engineering. United States.
- [11] FEMA. (2009). *Quantification of building seismic performance factors*, FEMA P-695, Federal Emergency Management Agency. United States.
- [12] FEMA P-795. (2011). *Quantification of building seismic performance factors: Component Equivalency Methodology*, prepared by Applied Technology Council for the Federal Emergency Management Agency, Washington, D.C.
- [13] Nippon Steel Engineering, "Unbonded brace: basic design information," *Nippon Steel Engineering Co. Ltd.*, Building Construction and Steel Structures Div., Undated.

- [14] ANSI/AISC 341-16. (2016). *Seismic provisions for structural steel buildings*, American Institute of Steel Construction, Chicago, Illinois, USA.
- [15] Hou, H., Li, H., Qiu, C., and Zhang, Y. (2018). "Effect of hysteretic of SMAs on seismic behavior of self-centering concentrically braced frames". *Struct Control Health Monit*, 25(3), 1 -14, <https://doi.org/10.1002/stc.2110>
- [16] Abou-Elfath, H. (2017). "Evaluating the ductility characteristic of self-centering buckling-restrained shape memory alloy braces". *Smart Mater. Struct*, 26, 055020, <https://doi.org/10.1088/1361-665X/aa6abc>
- [17] Janke, L., Czaderski, C., Motavalli, M., and Ruth, J. (2005). "Application of shape memory alloys in civil engineering structures-Overview, limits and new ideas". *Materials and Structures*, 38, 578-592.
- [18] Cladera, A., Weber, B., Leinebach, C., Czaderski, C., Shahverdi, M., and Motavalli, M. (2014). "Iron-based shape memory alloys for civil engineering structures: an overview". *Construction and building materials*, 63, 281-293.